PHYSICS OF FLUIDS **24**, 126101 (2012)

Shock structure in shock-turbulence interactions

Diego A. Donzis[a)]
Department of Aerospace Engineering, Texas A&M University, College Station, Texas 77843, USA

(Received 22 August 2012; accepted 24 October 2012; published online 20 December 2012)

The structure of a shock wave interacting with isotropic turbulence is investigated. General principles of similarity scaling show that consistency with known physical limiting behavior requires incomplete similarity solutions where the governing non-dimensional parameters, namely, the Reynolds, convective, and turbulent Mach numbers (R_λ, M, and M_t, respectively), can be combined to reduce the number of similarity parameters that describes the phenomenon. An important parameter is found to be $K = M_t/R_\lambda^{1/2}(M-1)$ which is proportional to the ratio of laminar shock thickness to the Kolmogorov length scale. The shock thickness under turbulent conditions, on the other hand, is essentially a random variable. Under a quasi-equilibrium assumption, shown to be valid when $K^2 \ll 1$, analytical results are obtained for the first and second moments of the turbulent shock thickness, velocity gradient, and dilatation at the shock. It is shown that these quantities exhibit universal behavior in the parameter K with corrections in $M_t/(M-1)$, for velocity fields with arbitrary statistics. Excellent agreement is observed with available data from direct numerical simulations. Two-point statistics of velocity gradients at the shock show that the distribution of dilatation over the shock surface is determined by transverse structure functions of the incoming turbulence. The regimes of the interaction are also investigated. It is found that the appropriate parameter to delimit the different regimes is $M_t/(M-1)$. Flow retardation ahead of the shock is suggested as a mechanism for so-called broken shocks. © *2012 American Institute of Physics*. [http://dx.doi.org/10.1063/1.4772064]

I. INTRODUCTION

In many engineering and natural systems, turbulent flows interact with shock waves. Classical examples of such flows include supernovae explosions, supersonic aerodynamics and propulsion, inertial confinement fusion, shock wave lithotripsy, and volcanic eruptions. Due to the tremendous difficulties in understanding such complex flows, efforts have been directed to study the simplest canonical cases, for example, the interaction of isotropic turbulence with a normal shock.

The first theoretical approaches[1–3] idealized the problem as a linear one where the shock is a discontinuity and the incoming flow was characterized by a single wave, or a superposition of them. Within the theory, the characteristics of the waves after the shock can be computed analytically. This theory which is based on a modal decomposition of the linearized Euler equations, is commonly referred to as the linear interaction analysis (LIA). A particularly useful decomposition of the incoming field is that of Kovasznay[4] into vortical, acoustic, and entropy modes which evolve independently to first order. Since then, a number of other theoretical approaches have been developed to try to characterize and predict how a shock affects the evolution of velocity, vorticity, or other quantities of interest.[5–12] Except for rapid distortion theory (RDT), all other approaches treat the shock as a discontinuity and are, therefore, unsuited to study the influence of the turbulence on the internal structure of the shock. RDT, on the other hand, assumes that the shock has a finite width

a)donzis@tamu.edu.

though it is decoupled from turbulence fluctuations and the assumption of homogeneity may not be fully justified inside the shock.

Although LIA has had relative success over other approaches in predicting specific trends, evince from experiments and simulations have consistently shown[13] that characteristics of the turbulence not accounted for in the theoretical work mentioned above such as length or velocity scales, can strongly modify the outcome of the interaction. In light of this situation we have recently suggested[14] that the amplification of turbulence across the shock, for example, can be better understood as a function of a non-dimensional parameter which is a combination of Reynolds, convective, and turbulent Mach numbers and can be related to the ratio of shock thickness to Kolmogorov length scale.

It has also become increasingly clear that depending on the characteristics of the incoming flow, the shock surface can preserve a well defined structure given by a steep gradient or can undergo substantial deformations leading to "holes" across the shock where very smooth compressions or multiple weak compression waves can occur.[15,16] These have been referred to as the "wrinkled" or "broken" regimes, respectively, in the literature. It is natural to think that such a modification of the structure of the shock could have a first order effect on the behavior of the interaction. Therefore, it seems important to understand how the shock structure reacts to the incoming turbulence and the role of this effect on the interaction. Quantitatively, there is particular interest in how important characteristics of the shock scale with the governing non-dimensional parameters. This is our main thrust here.

One of the problems faced while attempting to understand the interaction is the lack of a suitable criterion of what delineates different regimes including the determination of what constitutes asymptotic states. These are important when comparison with linear theories, for example, are attempted. Without that rough guideline, we can come to varying conclusions from simulations and experiments. While we have suggested such a guideline in Ref. 14, no quantitative information about the shock structure was provided. In this paper we derive statistics of the shock thickness and maximum velocity gradient at the shock as well as their spatial distribution across the shock surface. In Sec. II, we use general principles of similarity scaling to show that similarity scaling relations appear to be of the second kind (also known as incomplete similarity solutions)[17] in which dependence on some parameters will not disappear even when those parameters are large or small. Analytical results pertaining the structure of the shock are obtained in Sec. III which agree and support the analysis based on similarity scaling arguments. The important non-dimensional parameter to characterize the shock is found to be the same as suggested in Ref. 14. The excellent agreement between the theoretical predictions proposed here and the limited data available is shown in Sec. IV. The structure of the shock surface and its relation with the incoming turbulence is discussed in Sec. V. The results are then discussed in Sec. VI in the context of the regime of the interaction. Conclusions are given in Sec. VII.

II. SHOCK STRUCTURE: SIMILARITY SCALING

Dimensional analysis and similarity scaling methods are powerful tools that have been useful in understanding complex phenomena.[17] The overall objective here is to determine the behavior of the shock by using the knowledge about the state of the turbulence ahead of it. The essence of the problem is sketched in Fig. 1. As a starting point, the turbulent field can be characterized by the following dimensional parameters: a length scale such as the integral scale L, a turbulent velocity scale such as the rms velocity u, the mean viscosity μ, the mean density ρ, and a temperature scale. For a perfect gas, the temperature, T, is directly related to the speed of sound $c = \sqrt{\gamma RT}$ (where γ is the ratio of specific heats and R the gas constant) which is commonly used in compressible flows. While the mean upstream velocity U is an important parameter, the difference $U - c$ is more relevant for present purposes since the shock strength depends on the relative velocity instead of the absolute value U. Although the thermal conductivity is an important parameter, it is not an independent parameter if the the Prandtl number is assumed constant.

If the flow is laminar, the Mach number upstream of the shock, $M = U/c$, determines the problem completely as all jump conditions can then be written in terms of M alone.[18] When the flow is turbulent, on the other hand, this is generally not possible.[19] This makes simulations of

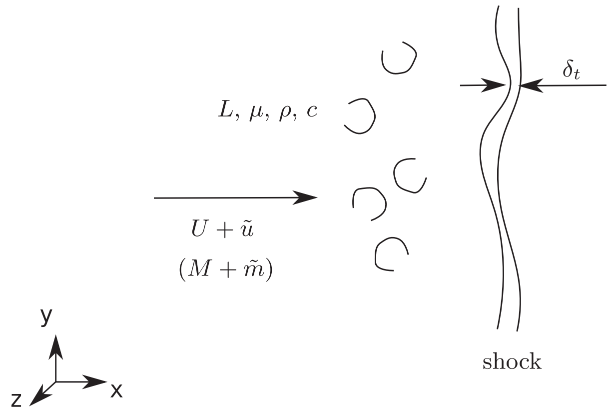

FIG. 1. Flow configuration: A statistically stationary shock interacts with isotropic turbulence convected at a mean velocity U and Mach number $M = U/c$ where c is the mean speed of sound. The turbulence is characterized by a large length scale L, a mean viscosity μ, and a mean density ρ. The fluctuating component of the velocity field is $\tilde{u}$ (the corresponding instantaneous Mach number is $\tilde{m} = \tilde{u}/c$); its rms is denoted by u. The shock thickness δ_t is a random variable that depends on y, z, and time.

stationary shocks more difficult since the boundary conditions necessary to maintain the *mean* location of a shock fixed in space (in particular the outflow pressure) cannot be estimated accurately in advance.[16,20] Still, the appropriate boundary conditions for a stationary shock are determined by the characteristics of the incoming turbulent flow.

We thus find, for a stationary shock, the following functional form:

$$\varphi = f(L, u, \mu, \rho, c, U - c), \tag{1}$$

where φ is a quantity of physical interest such as the velocity or vorticity fluctuations downstream of the shock, the thickness of the shock δ or other single-point statistics, and f is an unknown function.

Before we proceed further, a practical issue shall be clarified. Since the turbulence evolves (decays) as it approaches the shock, a specific location has to be identified to obtain the governing parameters in Eq. (1) in order to compare meaningfully geometrically similar flows. An obvious and natural choice is to use values immediately upstream of the shock wave, a convention used throughout the literature and hereafter.

Since there are six variables in Eq. (1) and only three with independent dimensions one can use dimensional analysis and reduce the number of parameters describing the phenomenon to three. By choosing μ, ρ, and c as the independent dimensions we find

$$\varphi^* = \Phi_\varphi(M_t, \Delta M, R_c), \tag{2}$$

where φ^* is the non-dimensional version of φ, Φ_φ is a universal function, and

$$M_t \equiv \sqrt{3}\frac{u}{c}, \quad \Delta M \equiv \frac{U - c}{c}, \quad R_c \equiv \frac{cL\rho}{\mu}\ . \tag{3}$$

The factor $\sqrt{3}$ for M_t is included for consistency with the widely used definition $M_t = \sqrt{u_i u_i}/c$ (summation implied). We note that the Reynolds number R_c is related to the most common $R_L \equiv uL\rho/\mu$ or the Taylor microscale Reynolds number $R_\lambda = u\lambda\rho/\mu$ (where λ is the Taylor microscale). The different definitions are related through $R_L = M_t R_c \approx {R_\lambda}^2$. The parameter ΔM is usually written in terms of the upstream Mach number $M = U/c$ as $\Delta M = M - 1$.

A. Laminar shock thickness: Incomplete similarity

After adopting a suitable definition for the shock thickness (to be made more precise below) one can write Eq. (2) as $\varphi^* = \delta/L = \Phi_\delta(M_t, \Delta M, R_c)$. Before considering the turbulent case, we note that under laminar conditions (for which a subscript l will be used), the quantities L and u have no physical meaning. Therefore, dimensional analysis applied to Eq. (1) results in

$$\delta_l = \frac{\mu}{\rho c}\Phi_{\delta l}(\Delta M). \tag{4}$$

From physical considerations, as ΔM increases, the shock thickness is expected to decrease. Conversely, when ΔM tends to zero, δ_l increases. Therefore, since in principle, $\Phi_{\delta l}$ does not approach a finite non-zero asymptotic value for ΔM very large or small, its dependence cannot be neglected *a priori* in either limit. If similarity is sought, only so-called *incomplete similarity* is possible and the dependence on ΔM must appear explicitly.[21] Assuming power-law asymptotics, we arrive at $\delta_l = C_l(\mu/\rho c)\Delta M^\sigma$ where C_l is a constant of order unity which will be dropped for simplicity, and the exponent σ must be negative to satisfy the asymptotic behavior mentioned above. This result is consistent with classical estimates using the Navier-Stokes equations[18] which predict $\sigma = -1$:

$$\delta_l \approx \frac{\mu}{\rho c}\frac{1}{\Delta M}. \tag{5}$$

Thus, the well-known scaling of the (laminar) shock thickness that can be obtained analytically from the governing equations, can also be derived using intermediate asymptotics as a case of incomplete similarity. This is clearly an asymptotic expression expected to be valid for small values of ΔM.

It is often useful to compare the shock thickness with turbulent length scales. Since the shock is typically thin compared to other flow scales, it is natural to compare δ_l with the smallest turbulent scale, that is the Kolmogorov scale $\eta = (\nu^3/\langle\epsilon\rangle)^{1/4}$ where $\langle\epsilon\rangle$ is the mean energy dissipation rate (angular brackets represent a suitably defined ensemble average). Within classical Kolmogorov[22] phenomenology, the velocity field is locally uniform at sub-Kolmogorov scales. Therefore, the comparison between δ_l and η reflects whether the shock, locally, is subjected to a uniform velocity field or its structure can interact with small-scale turbulence fluctuations. We will revisit this consideration below. The normalized shock thickness can now be written as

$$\frac{\delta_l}{\eta} \approx K \tag{6}$$

with K given by

$$K \equiv \frac{M_t^{3/4}}{R_c^{1/4}\Delta M} = \frac{M_t}{{R_\lambda}^{1/2}\Delta M} \tag{7}$$

written in terms of both R_c and R_λ. The latter scaling was already suggested in Ref. 23 and appears as an important parameter in other contexts.[24] The parameter K has also been recently suggested[14] to provide a universal description of amplification factors. With the help of Eq. (3) it is also possible to rewrite Eq. (6) as

$$\frac{\delta_l}{\eta} = \frac{u_\eta}{U - c}, \tag{8}$$

where $u_\eta = (\langle\epsilon\rangle\nu)^{1/4}$ is the Kolmogorov velocity scale which emphasizes the importance of the ratio of the characteristic velocity of the smallest turbulent scales and the relative velocity $U - c$. Thus for K close to unity, the Kolmogorov length scale is comparable to the laminar shock thickness and the Kolmogorov velocity scale is comparable to the mean velocity excess over sonic speeds. One can also compare δ_l with the integral scale by using $L \approx \eta {R_\lambda}^{3/2} = \eta(R_c M_t)^{3/4}$:

$$\frac{\delta_l}{L} \approx \frac{M_t}{{R_\lambda}^2\Delta M}. \tag{9}$$

B. Turbulent shock thickness: Incomplete similarity

Let us consider now the turbulent case of Eq. (2):

$$\frac{\langle\delta_t\rangle}{\eta} = \Phi_{\delta t}(M_t, \Delta M, R_c), \tag{10}$$

where the subscript t stands for turbulent and angular brackets (representing a suitably defined average) are explicitly written since the thickness is essentially a random variable in a turbulent flow (Fig. 1). In simulations of shock-turbulence interactions, a sensible choice of averages is over planes parallel to the shock surface.

Similar considerations to those for the laminar case apply here: for $\Delta M \to 0$ and $\Delta M \to \infty$, the ratio $\langle\delta_t\rangle/\eta$ is expected to tend to ∞ and 0, respectively. Furthermore, if $R_c \to \infty$ (e.g., in the limit of vanishing viscosity) the normalized shock thickness will tend to zero since the Kolmogorov scale decreases as $\mu^{3/4}$ (using the well-known property of dissipative anomaly[25]) while $\langle\delta_t\rangle$ is expected to behave (to first order) as μ. Conversely, we expect $\langle\delta_t\rangle/\eta \to \infty$ for $R_c \to 0$. Again, the non-finite asymptotic behavior suggests incomplete similarity, requiring retaining explicit dependence on these two similarity parameters. Assuming power law behavior for both, we arrive at

$$\frac{\langle\delta_t\rangle}{\eta} = \Delta M^{\alpha} R_c^{\beta} \Phi_{\delta t}\left(\frac{M_t}{\Delta M^{\alpha_1} R_c^{\beta_1}}\right), \tag{11}$$

where both α and β should be negative to be consistent with the limits mentioned above based on physical considerations. These exponents as well as α_1 and β_1 cannot be determined by dimensional arguments alone.

When the turbulent fluctuations are small, that is in the low-M_t limit, $\langle\delta_t\rangle/\eta$ is expected to tend to Eq. (6). To ensure this, we set $\alpha = -1$ and $\beta = -1/4$ and explicitly include[26] a factor $M_t^{3/4}$ so that the scaling function $\Phi_{\delta t}$ is multiplied by K:

$$\frac{\langle\delta_t\rangle}{\eta} = K\,\Phi_{\delta t}\left(\frac{M_t}{\Delta M^{\alpha_1} R_c^{\beta_1}}\right) \tag{12}$$

and require that $\Phi_{\delta t}(x) \to 1$ as $x \to 0$ thus assuring that $\langle\delta_t\rangle/\eta$ will tend to K when turbulence is sufficiently weak.

Although similarity analysis does not provide a functional form for the normalized shock thickness, it led to Eq. (12) which does constraint its form. In order to investigate the functional form of $\Phi_{\delta t}$ and whether this scaling is justified, we next turn to some analytical results on the shock structure.

III. ANALYTICAL RESULTS FOR THE SHOCK STRUCTURE

As already mentioned, the shock thickness δ_t is a function of space and time. We now assume that the internal structure of the shock is not modified by the turbulence and thus, locally, the thickness is given by the laminar solution. At each point, however, the fluctuating velocity (Mach number) is different and given by $M + \tilde{m}$ where $\tilde{m} = \tilde{u}/c$ and $\tilde{}$ stands for instantaneous fluctuations which depend on space and time (see Fig. 1). The normalized local shock thickness, δ_t^*, then, is given by

$$\delta_t^* \equiv \delta_t \frac{\rho c}{\mu} \approx \frac{1}{\Delta M + \tilde{m}} \tag{13}$$

as a result of Eq. (5) which is, then, also valid for relatively low Mach numbers. It is thus expected that in regions of high $\Delta M + \tilde{m}$, Eq. (13) will not be accurate. In particular, we expect thinner shocks than observed in experiments.[27]

If $f_{\tilde{m}}(\tilde{m})$, the probability density function (PDF) of $\tilde{m}$, is known, one can in principle obtain the PDF of δ_t^*, $f_{\delta_t^*}(\delta_t^*)$. A similar approach based on a weak-shock approximation has been used in Ref. 24 though the interest in that reference was in shocklets statistics in decaying isotropic turbulence in which case ΔM refers to the increment above unity of the shock Mach number measured in a shock-fixed frame of reference. In particular, their model is based on the strong assumption that jumps across the randomly distributed shocklets are the same as elsewhere in the flow. Such an assumption is not needed to obtain shock statistics in the present flow configuration and, as seen below, lead to different results.

Clearly, within the present model, avoiding negative thicknesses requires $|\tilde{m}| < \Delta M$—in other words, the PDF of $\tilde{m}$ has to have bounded support. A further requirement is that the PDF be symmetric if isotropy is assumed for the incoming turbulence.

Before proceeding further, it is important to assess whether Eq. (13) is able to faithfully capture the unsteady physics of the interaction. This will depend on whether the shock can adjust to new conditions at a faster time scale than all other time scales in the problem. In such a case, the shock is in equilibrium with instantaneous local conditions, and will, therefore, be referred to as a *quasi-equilibrium* assumption. Intuitively, this seems to be justified when changes occur over long time scales.[28] A formal investigation on the conditions under which the approximation is valid is developed in Appendix A. The main result is that quasi-equilibrium is appropriate when $K_t \ll 1$, where K_t is ratio of the shock time scale to the most disruptive turbulent perturbations. Since, as also shown in Appendix A, $K_t \approx K^2$ when ΔM is not too small, the condition for quasi-equilibrium is met when $K^2 \ll 1$, which is satisfied for most simulations and experiments in the literature.

A further comment is in order. In Eq. (13), $\tilde{m}$ was identified with the turbulent fluctuations of the incoming turbulence. However, the Mach number in Eq. (5) is based on the *relative* velocity between the flow and the shock wave. Thus, $\tilde{m}$ would contain contributions from both the turbulence and the shock motion. While not strictly necessary for the derivations that follow, we will assume, for simplicity in interpretation, that turbulent fluctuations are the dominant contributor. This may be further justified if the quasi-equilibrium assumption is satisfied, as the shock will quickly adjust to local conditions.

A. PDF and moments of shock thickness

Consider a velocity field characterized by a uniform distribution of the form

$$f_{\tilde{m}}(\tilde{m}) = \begin{cases} 1/(2m_1) & |\tilde{m}| \le m_1 \\ 0 & \text{otherwise} \end{cases}, \tag{14}$$

where m_1 is the maximum value $\tilde{m}$ can take. The turbulent Mach number M_t is then (see Eq. (3))

$$M_t = \sqrt{3}\left(\int \tilde{m}^2 f_{\tilde{m}}(\tilde{m})d\tilde{m}\right)^{1/2}, \tag{15}$$

which in the present case results in $M_t = m_1$. Using standard tools of probability,[29] it is easy to show from Eqs. (13) and (14), that

$$f_{\delta_t^*}(\delta_t^*) = \begin{cases} \frac{1}{2\delta_t^{*2}M_t} & (\Delta M + M_t)^{-1} \le \delta_t^* \le (\Delta M - M_t)^{-1} \\ 0 & \text{otherwise} \end{cases}. \tag{16}$$

Both $f_{\tilde{m}}(\tilde{m})$ and $f_{\delta_t^*}(\delta_t^*)$ are shown in Fig. 2. It can be seen that a wide range of values of δ_t (even wider than for $\tilde{u}$), around what is usually considered the nominal shock thickness given by Eq. (5), results from the interaction.

To compare the predictions of this model with the similarity analysis leading to Eq. (12), we can now use $f_{\delta_t^*}(\delta_t^*)$ to compute the normalized mean shock thickness as

$$\langle \delta_t^* \rangle = \int \delta_t^* f_{\delta_t^*}(\delta_t^*) d\delta_t^* = \tanh^{-1}(M_t/\Delta M)/M_t. \tag{17}$$

The (unnormalized) mean shock thickness $\langle \delta_t \rangle = \langle \delta_t^* \rangle \mu/\rho c$ can now be compared to the Kolmogorov length scale ($\eta \approx L R_L^{-3/4}$). The result is

$$\frac{\langle \delta_t \rangle}{\eta} = \frac{1}{M_t^{1/4} R_c^{1/4}} \tanh^{-1}(M_t/\Delta M). \tag{18}$$

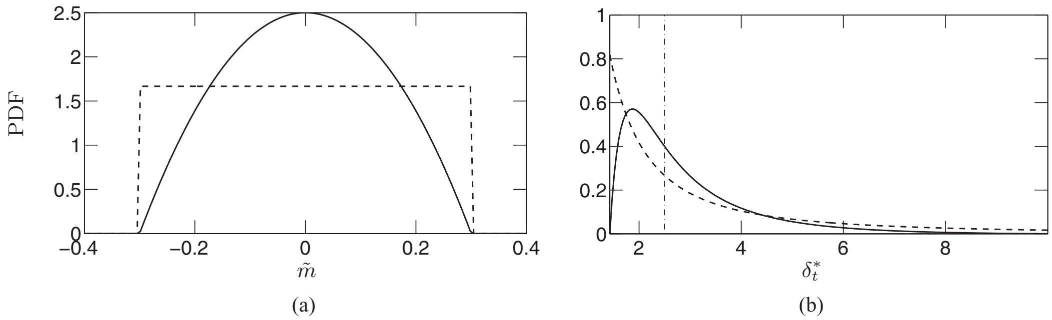

FIG. 2. (a) Model PDFs for velocity fluctuations upstream of the shock, $f_{\tilde{m}}(\tilde{m})$. Dashed and solid lines: uniform and Beta(α,β) distributions ($\alpha = \beta = 2$), respectively. (b) Resulting PDFs for normalized shock thickness $\delta_t^* = \delta_t \rho c/\mu$. Vertical dash-dotted line: nominal laminar shock thickness $\delta_t^* = 1/\Delta M$. For both PDFs, $m_1 = 0.3$ and $\Delta M = 0.4$.

Finally, a Taylor series expansion in M_t results in

$$\begin{aligned}\frac{\langle\delta_t\rangle}{\eta} &= \frac{M_t^{3/4}}{\Delta M R_c^{1/4}} + \frac{M_t^{11/4}}{3\Delta M^3 R_c^{1/4}} + \frac{M_t^{19/4}}{5\Delta M^5 R_c^{1/4}} + \ldots \\ &= K\left[1 + \frac{1}{3}\frac{M_t^2}{\Delta M^2} + \frac{1}{5}\frac{M_t^4}{\Delta M^4} + \frac{1}{7}\frac{M_t^6}{\Delta M^6} + \ldots\right].\end{aligned} \tag{19}$$

Clearly this expression agrees with the scaling of Eq. (12) derived from similarity scaling reasoning. The resulting scaling function is $\Phi_{\delta t} = 1 + (1/3)(M_t/\Delta M)^2 + (1/5)(M_t/\Delta M)^4 + \ldots$. This result, thus, supports incomplete similarity in ΔM and R_c assumed in Sec. II B. A direct comparison between Eqs. (19) and (12) reveals $\alpha_1 = 1$ and $\beta_1 = 0$.

While the mean value provides important information, further understanding of the structure of the shock can be gained by studying higher-order moments. For example, the second-order moment is $\langle\delta_t^{*2}\rangle = \int \delta_t^{*2} f_{\delta_t^*}(\delta_t^*) d\delta_t^*$, which, for the model in Eq. (14), yields $\langle\delta_t^{*2}\rangle = (\Delta M^2 - M_t^2)^{-1}$. If, as before, we normalize it by Kolmogorov length scale and expand the result as a series in M_t, we obtain

$$\frac{\langle\delta_t^2\rangle}{\eta^2} = K^2\left[1 + \frac{M_t^2}{\Delta M^2} + \frac{M_t^4}{\Delta M^4} + \frac{M_t^6}{\Delta M^6} + \ldots\right]. \tag{20}$$

In addition to the PDF model in Eq. (14), we have investigated the behavior of the turbulent shock thickness for velocity fields characterized by different PDFs, including distributed Dirac deltas, triangular and Betas distributions, and a truncated Gaussian (to satisfy the bounded support constraint). The particular case of a Beta distribution $B(\alpha, \beta)$ with parameters $\alpha = \beta = 2$ in the interval $[-m_1, m_1]$, is treated in Appendix B and the results included also in Fig. 2 to highlight that, as expected, the shape of the PDF of δ_t^* depends on the particular $f_{\tilde{m}}(\tilde{m})$ adopted. However, the mean turbulent thickness presents the following scaling for all PDFs:

$$\frac{\langle\delta_t\rangle}{\eta} = K\left[1 + a_1\frac{M_t^2}{\Delta M^2} + a_2\frac{M_t^4}{\Delta M^4} + a_3\frac{M_t^6}{\Delta M^6} + \ldots\right], \tag{21}$$

where $a_1 = 1/3$ and the numerical value of the coefficients $a_2, a_3, \ldots$ depend on the particular form of $f_{\tilde{m}}(\tilde{m})$ (compare Eqs. (19) and (B3)). All PDFs also show second-order moments that present the following scaling with the governing parameters:

$$\frac{\langle\delta_t^2\rangle}{\eta^2} = K^2\left[1 + b_1\frac{M_t^2}{\Delta M^2} + b_2\frac{M_t^4}{\Delta M^4} + b_3\frac{M_t^6}{\Delta M^6} + \ldots\right], \tag{22}$$

where $b_1 = 1$ and the rest of the coefficients depend on $f_{\tilde{m}}(\tilde{m})$. As we show next, the universal scaling of the shock thickness (in the sense of being the same for all velocity fields) is the result of the functional form relating $\tilde{m}$ and δ_t^* in Eq. (13). This can be seen if the mean of δ_t^* is written in terms of the PDF of $\tilde{m}$,

$$\langle \delta_t^* \rangle = \int g(\tilde{m}) f_{\tilde{m}}(\tilde{m}) d\tilde{m}, \tag{23}$$

where $g(\tilde{m}) = \delta_t^* = 1/(\Delta M + \tilde{m})$. If $g(\tilde{m})$ is expanded as a Taylor series around the mean $\langle \tilde{m} \rangle$ (which is zero in our case), the result is $g(\tilde{m}) = g(\langle \tilde{m} \rangle) + g'(\langle \tilde{m} \rangle)(\tilde{m} - \langle \tilde{m} \rangle) + g''(\langle \tilde{m} \rangle)(\tilde{m} - \langle \tilde{m} \rangle)^2/2 + \ldots$ (prime stands for derivative). When this expression is substituted into Eq. (23), upon integration, the second term on the right-hand-side vanishes by definition of the mean and the third term results in the variance of $\tilde{m}$, which is equal to $M_t^2/3$ according to Eq. (15). Furthermore, since $g''(\langle \tilde{m} \rangle) = 2/(\Delta M)^3$, we find to leading order

$$\begin{aligned} \langle \delta_t^* \rangle &= g(\langle \tilde{m} \rangle) + g''(\langle \tilde{m} \rangle) M_t^2/6 + \ldots \\ &= \frac{1}{\Delta M} + \frac{1}{3} \frac{M_t^2}{\Delta M^3} + \ldots, \end{aligned} \tag{24}$$

which, when normalized by Kolmogorov scale, can be written as

$$\frac{\langle \delta_t \rangle}{\eta} = K \left[1 + \frac{1}{3} \frac{M_t^2}{\Delta M^2} + \ldots \right] \tag{25}$$

a scaling in agreement with the results for different velocity fields and the similarity scaling analysis in Eq. (12). Thus, we have shown that regardless of the particular shape of the PDF of the incoming velocity field, to leading order, the mean shock thickness is given by Eq. (25).

Equation (25) (or (21)) provides some insight into the effect of turbulence on the shock thickness. First, it suggests that, to leading order, the normalized turbulent thickness is the same as the normalized laminar thickness (i.e., K). Second, for larger turbulent Mach numbers, the shock thickens relative to the Kolmogorov length scale with the parameter $M_t/\Delta M$ independent of the Reynolds number. Third, because the first coefficient of the expansion in Eq. (21) is known for all velocity fields, it is possible to quantify how small turbulent fluctuations must be in order for $\langle \delta_t \rangle$ to remain within some fraction of the laminar solution (i.e., $M_t^2/\Delta M^2/3$ can be bound to some fraction of unity).

A similar analysis can be carried for the second-order moment of the shock thickness $\langle \delta_t^2 \rangle$. In this case

$$\langle \delta_t^{*2} \rangle = \int g(\tilde{m})^2 f_{\tilde{m}}(\tilde{m}) d\tilde{m}. \tag{26}$$

We now expand $g(\tilde{m})^2$ around $\langle \tilde{m} \rangle$ and insert the resulting expression into Eq. (26), to obtain

$$\begin{aligned} \langle \delta_t^{*2} \rangle &= g(\langle \tilde{m} \rangle)^2 + [g'(\langle \tilde{m} \rangle)^2 + g(\langle \tilde{m} \rangle) g''(\langle \tilde{m} \rangle)] M_t^2/3 + \ldots. \\ &= \frac{1}{\Delta M^2} + \frac{M_t^2}{\Delta M^4} + \ldots. \end{aligned} \tag{27}$$

After normalizing by η^2, we can finally write

$$\frac{\langle \delta_t^2 \rangle}{\eta^2} = K^2 \left[1 + \frac{M_t^2}{\Delta M^2} + \ldots \right], \tag{28}$$

which is in agreement with Eq. (22).

Equations (25) and (28) show that, to leading order the behavior of the turbulent shock thickness is independent of the specific PDF of the incoming flow, as long as the second order moment (i.e., M_t) is the same. The same universal behavior is observed for the variance of the shock thickness which follows from previous results and the equality $\sigma_{\delta_t}^2 = \langle \delta_t^2 \rangle - \langle \delta_t \rangle^2$,

$$\frac{\sigma_{\delta_t}^2}{\eta^2} = K^2 \left[\frac{1}{3} \frac{M_t^2}{\Delta M^2} + \ldots \right], \tag{29}$$

showing that while the mean turbulent shock thickness increases with K in the low-M_t limit, the distribution around that mean, widens in proportion to $M_t^2/\Delta M^2$, a result consistent with qualitative observations[16] as shown below. We can further compute the rms-to-mean ratio $\Delta \equiv \sigma_{\delta_t}/\langle\delta_t\rangle$ with the help of Eqs. (25) and (29):

$$\Delta = d_1 \frac{M_t}{\Delta M} + d_2 \frac{M_t^3}{\Delta M^3} + \ldots, \tag{30}$$

where $d_1 = 1/\sqrt{3}$ and d_2 depends on the PDF of the incoming turbulence.

It is interesting to note that while moments of the shock thickness normalized by the Kolmogorov scale in our flow configuration depend on Reynolds and Mach numbers, Ref. 24 suggests that the statistics of shocklet thicknesses in isotropic turbulence do not. For example, the most probable shock thickness was found to be a constant when normalized by the mean Kolmogorov length scale. In the present case, on the other hand, not only it depends on R_λ, M_t and ΔM (see, e.g., Eq. (25)) but also on the PDF of the incoming flow (see, e.g., Fig. 2 and Appendix B), As mentioned above, in addition to the absence of a mean flow, a strong assumption in Ref. 24 is that the velocity jumps across shocklets is the same as velocity increments everywhere, whose PDF is further assumed to be independent of M_t.

IV. SHOCK STRUCTURE: DATA FROM NUMERICAL SIMULATIONS

To assess the predictions in Secs. II– III, one would need to compare the various expressions with shock-resolving direct numerical simulations (DNS) or experiments where the details of the shock structure are accurately resolved. Unfortunately, there is very scarce information of the structure of the shock in turbulent flows due to well-known resolution constraints in both experiments[13] and simulations.[30] The limited data comes exclusively from simulations where obtaining statistics inside the shock is, in principle, no more difficult than in other regions as long as the shock is resolved by the computational grid. Yet, resolving the shock in a simulation may be prohibitively computationally expensive and studies have either chosen ranges of parameters that lead to a relatively thick shock (e.g., low M and low R_λ) or used shock-capturing schemes which do not resolve the shock completely.

Here we will consider the data from Refs. 16 and 31 which represent the two cases mentioned above. The simulations in Ref. 16 cover a relatively wide range of turbulent and convective Mach numbers using shock-capturing schemes which makes a clear definition of the structure of the shock somewhat difficult.[32] Since shocks are only numerically captured, these simulations may be referred to as turbulence-resolving DNS. Data from Ref. 31, on the other hand, do resolve the shock but there is only one combination of (low) Reynolds and Mach numbers. In addition, neither of them present data for the shock thickness and inferences are to be made to compare with the results here.

In Ref. 16, the instantaneous dilatation at the shock ($\tilde{\theta}$, defined as the location where the dilatation takes the greatest negative value) was calculated for a range of M_t and ΔM to estimate the rms-to-mean ratio

$$\Theta \equiv \frac{\langle(\tilde{\theta} - \langle\tilde{\theta}\rangle)^2\rangle^{1/2}}{\langle\tilde{\theta}\rangle} = \left(\frac{\langle\tilde{\theta}^2\rangle}{\langle\tilde{\theta}\rangle^2} - 1\right)^{1/2}, \tag{31}$$

where angular brackets denote averages over the shock surface.

The quantity Θ has an important physical meaning. When this quantity is small, deviations from the mean dilatation are small and one expects the shock to retain its identity across the entire shock surface with a steep compression comparable to the laminar case of Eq. (6). For large Θ, on the other hand, a range of thicknesses will be present making the shock less identifiable with a singularity as it will comprise smooth or multiple compressions in increasingly large areas. These two asymptotic cases are commonly referred to as the wrinkled and broken regimes of the interaction, respectively[15,16] (Ref. 33 referred to these as "peaked" and "rounded" waves). While in some previous studies the transition from these regimes was determined by visual inspection of instantaneous pressure or density profiles, Ref. 14 suggested a transition governed by the parameter K which has also appeared here naturally as an important similarity parameter determining the behavior of the shock structure. As suggested below, though, another mechanism for broken shocks results in a criterion based on a different parameter.

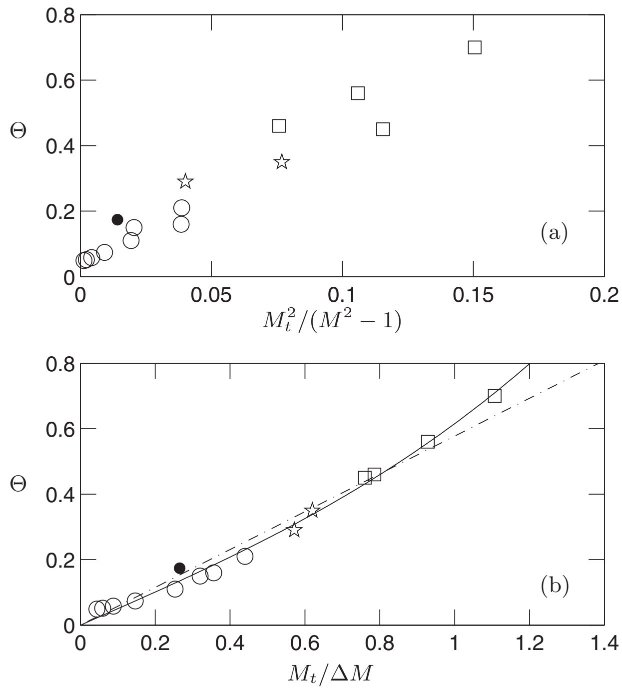

FIG. 3. (a) Normalized rms of dilation at the shock from Ref. 16 at $R_\lambda \approx 40$ (open symbols) and Ref. 31 at $R_\lambda \approx 5.5$ (closed symbol). (b) Same but as a function of the parameter $M_t/\Delta M$. Dashed-dotted line: Eq. (35). Dashed line: best fit for Eq. (37) with $e_1 = 0.502$ and $e_2 = 0.114$. Circles and squares: wrinkled and broken regimes, respectively, as defined in Ref. 16. Stars correspond to the intermediate state between the two.

We stress that while data from the shock-resolving simulations in Ref. 15 offer a more reliable representation of the shock, data from Ref. 16 present some challenges in interpretation due to the use of a shock-capturing scheme where the shock is not actually resolved by the grid. Nevertheless, the authors argued that in Eq. (31), the normalization of gradients by their mean value reduces, in part, the dependence on grid spacing. In lack of more reliable data from shock-resolving simulations we proceed, with this caveat, to compare our predictions with the data available.

In Fig. 3(a) we show Θ from Refs. 16 and 31 as a function of $M_t^2/(M^2-1)$ which has been previously suggested[15] to be an indicator of the regime of the interaction. The different symbols in the figure demark the different regimes as determined in Ref. 16. Despite the scatter, the data appear to follow the expected trend: small and large values of Θ are related to the wrinkled and broken regimes, respectively. However, we observe multiple values of Θ (even in different regimes) for a given $M_t^2/(M^2-1)$ which suggests that the latter may not be the appropriate parameter.

To compare with the results in Sec. III, we note that the shock thickness can be defined by means of the maximum negative velocity gradient in the streamwise direction $|\partial u/\partial x|_{max}$ which will be denoted by $|u_{x,max}|$ for short: $\delta_t \sim [u]/|u_{x,max}|$ where $[u]$ is the velocity jump across the shock. Since $u_{x,max}$ is the dominant component of the dilatation at the shock, instantaneously, we obtain $\tilde{\theta} \sim [u]/\delta_t$. Therefore, by writing $\tilde{\theta} \sim [u]\delta_t^{-1} = [u](\delta_t^* \mu/\rho c)^{-1} = [u](\rho c/\mu)(\Delta M + \tilde{m})$, we find the mean of the dilatation at the shock as

$$\langle \tilde{\theta} \rangle \approx \int [u] \frac{\rho c}{\mu} (\Delta M + \tilde{m}) f_{\tilde{m}}(\tilde{m}) d\tilde{m}. \tag{32}$$

If the effects of fluctuations on $[u]$ are neglected, to leading order, we find

$$\langle \tilde{\theta} \rangle \approx [u] \frac{\rho c}{\mu} \int (\Delta M + \tilde{m}) f_{\tilde{m}}(\tilde{m}) d\tilde{m} = [u] \frac{\rho c}{\mu} \Delta M. \tag{33}$$

Similarly, the second-order moment results in

$$\langle\tilde{\theta}^2\rangle = \left([u]\frac{\rho c}{\mu}\right)^2 \int (\Delta M + \tilde{m})^2 f_{\tilde{m}}(\tilde{m}) d\tilde{m} = \left([u]\frac{\rho c}{\mu}\right)^2 \left(\Delta M + \frac{M_t^2}{3}\right). \tag{34}$$

Finally, substituting these results into Eq. (31) yields,

$$\Theta \approx \frac{1}{\sqrt{3}} \frac{M_t}{\Delta M}. \tag{35}$$

This result is important because it suggests a new parameter on which Θ depends, namely, $M_t/\Delta M$. To test this we show, in Fig. 3(b), the data as a function of $M_t/\Delta M$. Comparison with part (a) in the figure, shows that the agreement is very satisfactory as all the data seem to collapse into a single curve. The figure also includes Eq. (35) (dashed-dotted line) which represents the data well even though departures are observed at high $M_t/\Delta M$. This, however, is not surprising. Since changes in $[u]$ were neglected, this expression is to be taken as a first-order approximation and can be expected to hold only for relatively small values of $M_t/\Delta M$.

We note that departures at higher Mach numbers may also be expected due to the use of the weak-shock approximation Eq. (13). However, a quantity like Θ may be less sensitive to this than unnormalized quantities (such as $\langle\delta_t\rangle$ or $\langle\delta_t^2\rangle$) since both the numerator and denominator in Eq. (31) may be affected in similar ways.

A more general approach is to use the actual analytical solution for the maximum negative gradient at the shock. Classical laminar calculations[18] show that

$$u_{x,max} = k_1[u]^2, \tag{36}$$

where $k_1 = -(\gamma + 1)/8D$, $D = (\mu/\rho)(4/3 + \mu_v/\mu + (\gamma - 1)/Pr)$, μ_v is the bulk viscosity, Pr is the Prandtl number and, within our set of assumptions, the instantaneous velocity jump is given by $[u] = -2c/(\gamma + 1)[(\Delta M + 1 + \tilde{m}) - 1/(\Delta M + 1 + \tilde{m})]$. The statistical moments of $u_{x,max}$ can now be estimated following the procedures used above. That is, with Eq. (36) and the PDF of $\tilde{m}$, we can compute $\langle u_{x,max}\rangle$ and $\langle u_{x,max}^2\rangle$, then expand in series around the mean to finally approximate $\Theta \approx (\langle u_{x,max}^2\rangle/\langle u_{x,max}\rangle^2 - 1)^{1/2}$ as

$$\Theta \approx e_1 \frac{M_t}{\Delta M} + e_2 \frac{M_t^3}{\Delta M^3} + \cdots, \tag{37}$$

where $e_1 = 1/\sqrt{3}$ consistent with Eq. (35). Equation (37), however, provides the next term of the expansion.

To test this result, Fig. 3(b) also shows a best fit of the form of Eq. (37) as a solid line with coefficients $e_1 \approx 0.502$ and $e_2 \approx 0.114$. We note that the best-fit value of the linear coefficient e_1 is close to the analytical value of $1/\sqrt{3}$ found in our analysis. Equation (37) clearly provides a better representation of the data for a wider ranger of $M_t/\Delta M$.

The scaling of Θ with $M_t/\Delta M$ can also be intuitively understood on physical grounds. If $\Theta = 0$ (which means a single value of the maximum velocity gradient for the entire shock) we expect $\Delta = 0$ (which means a single value of the thickness). More generally, when the PDF of δ_t widens, so does the PDF of $\tilde{\theta}$. Thus one can expect, $\Theta = \Phi_\Theta(\Delta)$ where Φ_Θ is an unknown function. Since Δ is a function of $M_t/\Delta M$ we thus have $\Theta \approx \Phi_\Theta^*(M_t/\Delta M)$. Furthermore, comparing Eq. (37) with Eq. (30) suggests that the function Φ_Θ is simply a multiplicative factor, i.e., $\Theta \approx k_2\Delta$ where k_2 is a constant which is close to unity.

We close this section by stressing that even though good agreement is seen between theoretical predictions and numerical data, most of the latter comes from shock-capturing simulations. Thus, while agreement is also seen for shock-resolving simulations (Fig. 3), a more definite conclusion in this regard must await comparison with fully resolved simulations at a wider range of Mach and Reynolds numbers, not yet available in the literature.

V. STRUCTURE OF SHOCK SURFACE

The results from Secs. II– IV dealt with single-point moments of the shock thickness and velocity gradients when the incoming turbulence is characterized by single-point statistics only. In other words, the turbulence has no spatial structure. In this section we extend the results to two-point statistics capturing some of the structural characteristics of the incoming turbulence. Let us consider again Eq. (13) but in the following form:

$$\tilde{m} = \delta_t^{*-1} - \Delta M. \tag{38}$$

A similar equation can be written at a different location over the shock (denoted with primes) which can be subtracted from Eq. (38):

$$\tilde{m} - \tilde{m}' = \delta_t^{*-1} - \delta_t^{*\prime -1}. \tag{39}$$

Squaring both sides and taking plane averages yields

$$D_u^T(\mathbf{r})/c^2 = D_w(\mathbf{r})\mu^2/\rho^2 c^2, \tag{40}$$

where $D_u^T(\mathbf{r}) \equiv \langle (\tilde{u} - \tilde{u}')^2 \rangle$ is identified as a transverse second-order structure function since the separation vector $\mathbf{r}$ (which lies on a plane parallel to the shock) is normal to the velocity component $\tilde{u}$. The function $D_w(\mathbf{r})$ is defined similarly as $D_w(\mathbf{r}) \equiv \langle (w - w')^2 \rangle$ where, for simplicity, we set $w \equiv 1/\delta_t$. Just as $D_u^T(r)$ provides information about the structure of the incoming turbulence (including spectral content), the structure function of w provides a sense of the spatial structure of the shock surface. Furthermore, $D_w(r)$ provides information also about the maximum negative gradient and dilatation at the shock since $w = 1/\delta_t \sim |u_{x,max}| \sim \tilde{\theta}$ when the velocity jump $[u]$ is considered unaffected by turbulent fluctuations (see Sec. IV).

If the upstream turbulence is isotropic (or axisymmetric) the direction of $\mathbf{r}$ is irrelevant (as long as it is parallel to the shock surface) and structure functions will depend on $r = |\mathbf{r}|$ only. We then write Eq. (40) as $D_w(r) = \rho^2/\mu^2 D_u^T(r)$ which provides a link between the structure of the shock surface and the turbulence ahead of it.

According to the classical phenomenology of Kolmogorov[22] the normalized structure function $D_u^T(r)/u_\eta^2 = h(r/\eta)$ is a universal function of r/η. If corrections due to intermittency and the bottleneck effect[34] are neglected, we can then rewrite Eq. (40) as

$$D_w(r/\eta)\eta^2 = h(r/\eta). \tag{41}$$

The scaling of $h(r/\eta)$ is relatively well understood. For small separations transverse velocity increments can be represented by a Taylor series which to first order yields $h(r/\eta) = (2/15)(r/\eta)^2$. At larger scales but still smaller than the integral length scales (the inertial range), Kolmogorov scaling (K41) predicts $h(r/\eta) = c_K^T(r/\eta)^{2/3}$. Finally, at the largest separations, the correlation between the velocity at two points vanishes and $h(r/\eta)$ approaches a constant value of $2u^2/u_\eta^2$. We thus have

$$D_w(r/\eta)\eta^2 = \begin{cases} (2/15)(r/\eta)^2 & r \ll \eta \\ c_K^T(r/\eta)^{2/3} & \eta \ll r \ll L \\ 2u^2/u_\eta^2 & L \ll r \end{cases}. \tag{42}$$

At very high Reynolds numbers, a wide inertial range develops where the $r^{2/3}$ scaling corresponds to $k^{-5/3}$ in spectral space.[35] Therefore, the distribution of thicknesses (and peak dilatation at the shock) will be characterized by a $k^{-5/3}$ scaling in wavenumber space. At moderate Reynolds numbers, however, the inertial range is very narrow. Moreover, the asymptotic inertial-range scaling for the *transverse* spectrum (which is the one related to the spatial structure of the shock surface) may require higher Reynolds numbers than for the longitudinal counterpart.[36]

Related to the structure function is the auto-correlation function defined as $R_w(r) = \langle (w - \langle w \rangle)(w' - \langle w' \rangle) \rangle / \sigma_w^2 = (\langle w w' \rangle - \langle w \rangle^2)/\sigma_w^2$, where $\sigma_w^2 = \langle (w - \langle w \rangle)^2 \rangle = \langle w^2 \rangle - \langle w \rangle^2$ is the variance of w (as well as of w' due to homogeneity in the two transverse directions). It is then relatively easy to show that

$$R_w(r) \approx R_u^T(r), \tag{43}$$

where $R_u^T(r)$ is the transverse correlation function for the streamwise velocity component. An important implication of this result is that the integral length scales of the shock and the turbulence (which are the integral of the respective correlation functions) are commensurate. We point out, however, that behind the shock, information propagating at the speed of sound can create long-range correlations which are not accounted for in the present analysis. Therefore, larger integral length scales cannot be ruled out.

VI. REGIME OF THE INTERACTION

As mentioned in Sec. I, it has been recognized that the interaction could be in different regimes depending on whether the shock remains a sharp gradient across the entire surface or it is greatly distorted leading to smooth compressions or multiple compression waves along individual streamlines. These have been referred to as wrinkled and broken (or peaked and rounded) regimes,[16,33] respectively. Since their definition has been typically based on visual inspections of instantaneous contours of pressure or density, in Ref. 14 we have suggested that the parameter K can be used to quantitatively assess some of the characteristics of the interaction: low-K interactions correspond to well-defined fronts while high-K interactions correspond to more distorted shocks. The transition, however, was found to be smooth for amplification factors of streamwise velocity components (G_{u^2}) with a scaling of the form $G_{u^2} \sim 0.75K^{-1/4}$ and a specific value of K to delimit different regimes would carry some degree of arbitrariness. Below, a different mechanism is proposed which results in a transition that depends on $M_t/\Delta M$ instead.

Intuitively, holes may appear when velocity fluctuations are such that at some location the local Mach number is less than unity. This possibility is consistent with observations[16] that smooth compressions appear to be correlated with retardation of the flow ahead of the shock. The conditions necessary for this to happen can be estimated by considering that the velocity field at large scales obeys Gaussian statistics which is, in fact, a good approximation.[35] The probability of $\Delta M + \tilde{m} < 0$ (a locally subsonic flow) is then $P_s \equiv P(\tilde{m} < -\Delta M) = (1 - \mathrm{erf}(\Delta M/\sqrt{2}\sigma))/2$ where erf(.) is the error function and σ is the standard deviation of $\tilde{m}$ which can be written as $\sigma = M_t/\sqrt{3}$. Then, $P_s = [1 - \mathrm{erf}(\sqrt{3/2}\frac{1}{M_t/\Delta M})]/2$. For $M_t/\Delta M \approx 0.6$ (as taken from Fig. 3(b)) the probability of such subsonic events is 0.0019. In other words, less than 0.2% of the surface will be subjected to subsonic velocities. For the strongest case in the figure (largest $M_t/\Delta M$) the probability is about 6%. It is interesting to note that, as seen in Fig. 4, P_s is negligible when $M_t/\Delta M$ is less than 0.6 and increases approximately linearly for larger values of $M_t/\Delta M$. The change of behavior of P_s at $M_t/\Delta M$ about

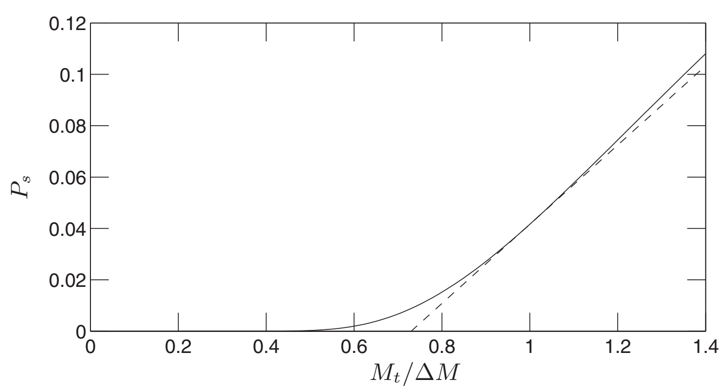

FIG. 4. Probability of flow being locally subsonic $P_s = P(\tilde{m} < -\Delta M)$ for Gaussian upstream turbulence. Dashed line: $(1 - \mathrm{erf}(\sqrt{3/2}))/2 + \sqrt{3/2\pi}(M_t/\Delta M - 1)/e^{3/2}$ which are the first terms in the Taylor expansion of P_s around $M_t/\Delta M = 1$.

0.6 agrees with the regimes as determined in Refs. 15 and 16. A similar result was recently suggested independently.[37]

The results of this analysis, however, do not depend on the Reynolds number. This is the consequence of assuming a Gaussian velocity field which has no associated length scales and therefore, no structure. The agreement with the data may then suggest a kinematic mechanism for broken shocks independent of Reynolds number.

We also note that for fixed Reynolds numbers, $M_t/\Delta M$ is proportional to K. If the alternative interpretation of K given by Eq. (8) is used, it is easy to see that values of K of order unity (or greater) corresponds to Kolmogorov velocities larger than the excess $U - c$. Because within K41 phenomenology, characteristic velocities decrease with scale, the situation $K \sim O(1)$ would imply that the velocities associated with all scales are larger than $U - c$ and massive subsonic regions should be expected. The analysis above, on the other hand, establishes the boundary between regimes based only on the most energetic scales. As K increases, smaller turbulent scales may be increasingly responsible for creating subsonic regions.

We finally make a note about the generality of the preceding results. The estimate Eq. (13) is strictly valid for small values of ΔM thus limiting, in principle, its applicability to weak shocks. However, if the appearance of subsonic regions is the leading cause of broken regimes, then only the local Mach number is important, and not the details of the shock structure. For local conditions close to sonic, Eq. (13) will be the appropriate approximation. Thus, the appearance of a broken regime based on locally subsonic regions is valid also for strong shocks.

VII. CONCLUSIONS

We have investigated the interaction of a shock wave with approximately isotropic turbulence. The prevailing theoretical approach used to attempt to understand data from experiments and simulations, is LIA which is formally valid in the high-R_c and low-M_t limits. From a similarity perspective, this corresponds to complete similarity in both Reynolds and turbulent Mach numbers which are further assumed to be sufficiently high and low, respectively. However, data from experiments and simulations consistently show dependence on these two parameters.

Using general principles of similarity analysis, it was found that only incomplete similarity solutions are consistent with known limiting behavior of the thickness of the shock. On this basis, the well-known laminar estimation δ_l using the Navier-Stokes equations was re-derived using similarity arguments. The ratio of laminar shock thickness to Kolmogorov scale was found to be $\delta_l/\eta = K$ with $K = M_t/R_\lambda{}^{1/2}\Delta M$. This ratio is also proportional to the ratio of Kolmogorov velocity scale, u_η, and the mean velocity excess $U - c$. For the turbulent case, the mean shock thickness was found to posses also incomplete similarity in the governing parameters reducing the relevant parameters from three to one. The physical importance of incomplete similarity is its implication that even if some parameters are very small (e.g., M_t) or very large (e.g., R_c), they cannot be neglected *a priori* and have to be accounted for to understand the different limiting behavior.[17]

Under the quasi-equilibrium assumption embodied in Eq. (13), which is shown to be valid when $K_t \approx K^2 \ll 1$, a number of analytical results have been obtained. Different velocity fields, characterized by different PDFs, result in different PDFs for shock thicknesses which present wider fluctuations around the mean than the velocity field that generate those fluctuations. However, the first two moments scale in a universal fashion as $\langle\delta_t\rangle/\eta \approx K[1 + (1/3)(M_t/\Delta M)^2 + \ldots]$ and $\langle\delta_t^2\rangle/\eta^2 \approx K^2[1 + (M_t/\Delta M)^2 + \ldots]$. These results support the similarity scaling analysis presented in Sec. II. Higher-order moments of the shock thickness, though, are likely to depend on high-order statistics of the turbulence velocity field as well.

The rms-to-mean-ratio of the dilatation at the shock was found to be given by $\Theta \approx (1/\sqrt{3})M_t/\Delta M + \ldots$ which agrees very well with DNS data for low values of $M_t/\Delta M$. For higher values, the next term in the expansion is found to be proportional to $M_t^3/\Delta M^3$ which extends the range of agreement to all data available. Thus, $M_t/\Delta M$ appears to be a better alternative to the parameter $M_t^2/(M^2 - 1)$ used in the literature.[15,16]

The analysis has also been extended to two-point statistics which provides information about the structure of the shock surface. The distribution of maximum gradients across the shock follows a $k^{-5/3}$ scaling in the inertial range of scales of the incoming turbulence. Obviously much higher Reynolds numbers that currently available are needed to discern a true inertial range. The integral scale associated with thicknesses or velocity gradients across the shock surface appear to be of the same order as the transverse integral length of turbulence though longer scales may be expected from pressure waves in the downstream region.

A mechanism for "holes" observed in shocks in the so-called broken regime was proposed based on locally subsonic regions. Results for a Gaussian velocity field, suggests a transition at $M_t/\Delta M \approx 0.6$ in agreement with Refs. 15 and 16. The determination of the precise mechanism leading to broken shocks will likely require detailed high-fidelity shock-resolving simulations at a range of values of ΔM, M_t, and R_λ not currently available.

ACKNOWLEDGMENTS

The author gratefully acknowledges support from NSF (Grant No. OCI-1054966) and AFOSR (Grant No. FA9550-12-1-0168). The author thanks helpful comments by S. K. Lele, J. Larsson, and S. Jamme as well as for the data from their simulations.

APPENDIX A: VALIDITY OF A QUASI-EQUILIBRIUM ASSUMPTION

Some results in Secs. III–V were based on the assumption that Eq. (13) is instantaneously valid—that is, the assumption that the shock wave is in quasi-equilibrium with local conditions. In principle, the validity of such a claim depends on how fast the shock can adjust to changing conditions. Thus, we now provide conditions under which a quasi-equilibrium approximation is valid.

Since the main mechanism for shock creation is the steepening process of non-linear inviscid terms it seems reasonable to estimate the time scale of this process using an inviscid approximation. For this, valuable information can be obtained by establishing how the velocity gradient evolves from some initial perturbation as one follows the wave that is created. Since this problem is analyzed in classical textbooks[38] we only include the main results needed here.

The interest is in the evolution of the velocity gradient u_x as ones follows the traveling wave, that is $[d(u_x)/dt]_{wave}$. In a one-dimensional isentropic setup it can be shown[38] that $[d(u_x)/dt]_{wave} = -(\gamma+1)u_x^2/2$ whose solution from some t_1 to $t_2 = t_1 + \Delta t$ is

$$u_x(t_2) = [u_x(t_1) + (\gamma+1)\Delta t/2]^{-1}. \tag{A1}$$

Clearly, if $u_x(t_1)$ is negative, gradients will steepen until $\Delta t = 2/|u_x(t_1)|(\gamma+1)$ where a discontinuity appears. Alternatively, the time between any two states, can be easily obtained from Eq. (A1) as

$$\Delta t = [2/(\gamma+1)]\left(u_x(t_2)^{-1} - u_x(t_1)^{-1}\right). \tag{A2}$$

For the problem of interest here, however, viscosity is not zero and gradients are limited by the smoothing effect of viscous forces. We are, therefore, interested in the time taken between two states determined by the competition between non-linear steepening and viscous effects. If we focus our attention on the maximum negative gradient (i.e., $u_x = u_{x,max}$), then the initial and final states are determined by Eq. (36). Let M and $M + \delta M$ represent these two states. Then combining Eq. (36) with Eq. (A2) yields

$$\Delta t = (4D/c^2)\left[(M - M^{-1})^{-2} - (M + \delta M - (M+\delta M)^{-1})^{-2}\right], \tag{A3}$$

which, when expanded as a Taylor series in δM, and neglecting numerical prefactors, can be written as

$$\Delta t \approx \frac{D}{c^2} g_1(M)\delta M + O(\delta M^2) \tag{A4}$$

with $g_1(M) = M(1+M^2)/(M^2-1)^3$. Equation (A4), thus, represents the time required for the shock to relax from M to $M + \delta M$.

Since turbulence is responsible for changes in the local Mach number, it is useful to relate δM to the characteristics of the incoming flow. In particular, these changes in M are produced by changes in the velocity over a streamwise distance r, that is $u(x+r) - u(x)$, as turbulence is convected towards the shock. We could now consider a typical fluctuation which will be of order $\sqrt{D_u^L(r)}$ where $D_u^L(r)$ is the second order longitudinal structure function. Therefore, we can estimate $\delta M = \sqrt{D_u^L(r)}/c$. We now need to consider the time scale at which such a perturbation is introduced. If turbulence is assumed to be swept by the mean flow at a mean velocity U, a perturbation $\delta M = \sqrt{D_u^L(r)}/c$ is convected through the shock in a time scale of order $\tau_c \approx r/U$.

We now proceed to compare the relevant times scales. If the convective time scale τ_c is much longer than the time needed for the shock wave to adjust to new conditions—Δt in Eq. (A4)—then the quasi-equilibrium assumption leading to Eq. (13) is justified. In other words, quasi-equilibrium is valid if

$$K_t \ll 1, \tag{A5}$$

where

$$K_t \equiv \frac{\Delta t}{\tau_c} \approx \frac{D}{c^2} g_1(M) \frac{\sqrt{D_u^L(r)}}{c} \frac{U}{r} . \tag{A6}$$

Since K_t depends on r, one could identify the worst case scenario—where K_t is maximum—and verify whether Eq. (A5) is satisfied. Clearly, the dependence on r is through $\sqrt{D_u^L(r)}/r$. By studying the longitudinal analogous to Eq. (42), it is possible to show that $\sqrt{D_u^L(r)}/r$ approaches a constant equal to $u_\eta/\eta\sqrt{15} = (\langle\epsilon\rangle/\nu)^{1/2}/\sqrt{15}$ at the smallest scales which provides the most severe test for Eq. (A5). We can then write

$$K_t \approx \frac{D}{c^2} g_1(M) M \frac{1}{\sqrt{15}} \left(\frac{\langle\epsilon\rangle}{\nu}\right)^{1/2} \approx \frac{\nu}{c^2} g_2(M) \frac{u}{\lambda}, \tag{A7}$$

where we have used the well-known relation $\langle\epsilon\rangle \sim \nu u^2/\lambda^2$ and the approximation $D \propto \mu/\rho = \nu$ which is valid for zero bulk viscosity (or constant μ_v/μ) and constant Prandtl number. We have also defined $g_2(M) \equiv g_1(M)M$.

A functional form that provides a good approximation for $g_2(M)$ for a wide range of values of M relevant to simulations[15,16,31,39–41] is $1/\Delta M^2$. While the high-M asymptote is correctly represented by this function some departures appear very close to $M = 1$ ($\Delta M = 0$) where an actual discontinuity grows with the third power of ΔM. Using this result into Eq. (A7) along with Eq. (7) and omitting all order-one factors, yields,

$$K_t \approx K^2. \tag{A8}$$

We therefore find that the condition $K_t \ll 1$ (necessary for quasi-equilibrium) is satisfied when $K^2 \ll 1$ which, in turn, represents the situation where the laminar shock thickness is smaller than the Kolmogorov length scale. It also corresponds to the case where the Kolmogorov velocity scale is smaller than the velocity excess $U - c$ (Eq. (8)). This is the case for all the data collected in Ref. 14. We note, however, that for very small values of ΔM, another factor $1/\Delta M$ reappears due to the singularity at $M = 1$. Therefore we have $K_t \approx K^2/\Delta M$ for $\Delta M \to 0$.

In summary, we have obtained an estimation of the conditions necessary for a quasi-equilibrium approximation—that is, the validity of Eq. (13) in an instantaneous basis—to hold. For this assumption to be valid, the shock wave must be able to adjust to local conditions at a much shorter time scale than those associated with the most disruptive turbulent perturbations. This is justified when $K_t \approx K^2 \ll 1$ (for ΔM not too small).

APPENDIX B: INCOMING TURBULENCE WITH A BETA DISTRIBUTION

The incoming velocity field in Fig. 1 can be modeled with a Beta distribution $B(\alpha, \beta)$ with parameters $\alpha = \beta = 2$ in the interval $[-m_1, m_1]$. This PDF is shown in Fig. 2(a). In this case, the

PDF of the normalized thickness is

$$f_{\delta_t^*}(\delta_t^*) = (9/20)\sqrt{3/5}(5M_t^2/3 - (1/\delta_t^* - \Delta M)^2)/(\delta_t^{*2} M_t^3) \tag{B1}$$

for $(\Delta M + \sqrt{5/3}M_t)^{-1} < \delta_t^* < (\Delta M - \sqrt{5/3}M_t)^{-1}$, shown in Fig. 2(b). The mean value is then

$$\langle \delta_t^* \rangle = \left[3\sqrt{15}\left(5{M_t}^2 - 3\Delta M^2\right)\tanh^{-1}\left(\sqrt{5/3}M_t/\Delta M\right) + 45\Delta M M_t\right]/(50{M_t}^3). \tag{B2}$$

When normalized with Kolmogorov length scale and expanded in powers of M_t, the mean shock thickness is given by

$$\frac{\langle \delta_t \rangle}{\eta} = K\left[1 + \frac{1}{3}\frac{M_t^2}{\Delta M^2} + \frac{5}{21}\frac{M_t^4}{\Delta M^4} + \ldots\right]. \tag{B3}$$

This form is essentially the same as Eq. (19) with slightly different coefficients. The second-order moment and variance of δ_t for this model are

$$\frac{\langle \delta_t^2 \rangle}{\eta^2} = K^2\left[1 + \frac{M_t^2}{\Delta M^2} + \frac{25}{21}\frac{M_t^4}{\Delta M^4} + \ldots\right], \qquad \frac{\sigma_{\delta_t}^2}{\eta^2} = K^2\left[\frac{1}{3}\frac{M_t^2}{\Delta M^2} + \frac{38}{63}\frac{M_t^4}{\Delta M^4} + \ldots\right], \tag{B4}$$

which are also of the same form as those resulting from the previous model of Eq. (14), with small difference in some of the coefficients. The most probable thickness normalized by Kolmogorov scale can be found from Eq. (B1) to be $({M_t}^{3/4}(\sqrt{9\Delta M^2 + 120{M_t}^2} - 9\Delta M))/(2{R_c}^{1/4}\left(5{M_t}^2 - 3\Delta M^2\right))$. This maximum can be also identified in Fig. 2(b).

[1] H. S. Ribner, "Shock-turbulence interaction and the generation of noise," NACA Report TR-1233 (1954).
[2] H. S. Ribner, "Convection of a pattern of vorticity through a shock wave," NACA Report TR-1164 (1954).
[3] F. K. Moore, "Unsteady oblique interaction of a shock wave with a plane disturbance," NACA Report TR-1165 (1954).
[4] L. S. G. Kovasznay, "Turbulence in supersonic flow," J. Aeronaut. Sci. **20**, 657–674 (1953).
[5] C. Truesdell, "On curved shocks in steady plane flow of an ideal fluid," J. Aeronaut. Sci. **19**, 826–828 (1952).
[6] M. J. Lighthill, "Dynamics of a dissociating gas. Part I. Equilibrium flow," J. Fluid Mech. **2**, 1–32 (1957).
[7] W. D. Hayes, "The vorticity jump across a gasdynamic discontinuity," J. Fluid Mech. **2**, 595–600 (1957).
[8] P. A. Durbin and O. Zeman, "Rapid distortion theory for homogeneous compressed turbulence with application to modeling," J. Fluid Mech. **242**, 349–370 (1992).
[9] L. Jacquin, C. Cambon, and E. Blin, "Turbulence amplification by a shock wave and rapid distortion theory," Phys. Fluids **5**, 2539–2550 (1993).
[10] G. P. Zank, Y. Zhou, W. H. Matthaeus, and W. K. M. Rice, "The interaction of turbulence with shock waves: A basic model," Phys. Fluids **14**, 3766–3774 (2002).
[11] X. Z. Ao, G. P. Zank, N. V. Pogorelov, and D. Shaikh, "Interaction of a thin shock with turbulence. I. Effect on shock structure: Analytic model," Phys. Fluids **20**, 127102 (2008).
[12] J. G. Wouchuk, C. H. R. de Lira, and A. L. Velikovich, "Analytical linear theory for the interaction of a planar shock wave with an isotropic turbulent vorticity field," Phys. Rev. E **79**, 066315 (2009).
[13] Y. Andreopoulos, J. H. Agui, and G. Briassulis, "Shock wave-turbulence interactions," Annu. Rev. Fluid Mech. **32**, 309–345 (2000).
[14] D. A. Donzis, "Amplification factors in shock-turbulence interactions: Effect of shock thickness," Phys. Fluids **24**, 011705 (2012).
[15] S. Lee, S. K. Lele, and P. Moin, "Direct numerical simulation of isotropic turbulence interacting with a weak shock wave," J. Fluid Mech. **251**, 533–562 (1993).
[16] J. Larsson and S. K. Lele, "Direct numerical simulation of canonical shock/turbulence interaction," Phys. Fluids **21**, 126101 (2009).
[17] G. I. Barenblatt, *Scaling* (Cambridge University Press, Cambridge, 2003).
[18] P. A. Thompson, *Compressible Fluid Dynamics* (McGraw Hill, New York, 1984).
[19] S. K. Lele, "Compact finite-difference schemes with spectral-like resolution," J. Comput. Phys. **103**, 16–42 (1992).
[20] N. Grube and M. P. Martin, "Numerical investigation of shock/isotropic turbulence interactions," AIAA Paper No. 2011–480 (2011).
[21] G. I. Barenblatt and Y. B. Zeldovich, "Self-similar solutions as intermediate asymptotics," Annu. Rev. Fluid Mech. **4**, 285–312 (1972).
[22] A. N. Kolmogorov, "Local structure of turbulence in an incompressible fluid for very large Reynolds numbers," Dokl. Akad. Nauk SSSR **30**, 299–303 (1941).
[23] P. Moin and K. Mahesh, "Direct numerical simulation: A tool in turbulence research," Annu. Rev. Fluid Mech. **30**, 539–578 (1998).
[24] R. Samtaney, D. I. Pullin, and B. Kosovic, "Direct numerical simulation of decaying compressible turbulence and shocklet statistics," Phys. Fluids **13**, 1415 (2001).
[25] K. R. Sreenivasan, "An update on the energy dissipation rate in isotropic turbulence," Phys. Fluids **10**, 528–529 (1998).

[26] This can be done by multiplying and dividing by $M_t^{3/4}$ and absorbing $1/M_t^{3/4}$ into $\Phi_{\delta t}$. This step is justified if $\Phi_{\delta t}$ consists of sums of monomials, since the exponents α_1 and β_1 are still unspecified.
[27] H. Alsmeyer, "Density profiles in argon and nitrogen shock waves measured by the absorption of an electron beam," J. Fluid Mech. **74**, 497–513 (1976).
[28] P. J. K. Bruce and H. Babinsky, "Unsteady shock wave dynamics," J. Fluid Mech. **603**, 463–473 (2008).
[29] A. Papoulis and S. U. Pillai, *Probability, Random Variables, and Stochastic Processes*, 4th ed. (McGraw-Hill, 2002).
[30] E. Johnsen, J. Larsson, A. V. Bhagatwala, W. H. Cabot, P. Moin, B. J. Olson, P. S. Rawat, S. K. Shankar, B. Sjögreen, H. C. Yee, X. Zhong, and S. K. Lele, "Assessment of high-resolution methods for numerical simulations of compressible turbulence with shock waves," J. Comput. Phys. **229**, 1213–1237 (2010).
[31] S. Jamme, J.-B. Cazalbou, F. Torres, and P. Chassaing, "Direct numerical simulation of the interaction between a shock wave and various types of isotropic turbulence," Flow, Turbul. Combust. **68**, 227–268 (2002).
[32] S. Pirozzoli, "Numerical methods for high-speed flows," Annu. Rev. Fluid Mech. **43**, 163–194 (2011).
[33] L. Hesselink and B. Sturtevant, "Propagation of weak shocks through a random medium," J. Fluid Mech. **196**, 513–553 (1988).
[34] D. A. Donzis and K. R. Sreenivasan, "The bottleneck effect and the Kolmogorov constant in isotropic turbulence," J. Fluid Mech. **657**, 171–188 (2010).
[35] A. S. Monin and A. M. Yaglom, *Statistical Fluid Mechanics* (MIT, 1975), Vol. 2.
[36] L. Mydlarski and Z. Warhaft, "On the onset of high-Reynolds-number grid-generated wind tunnel turbulence," J. Fluid Mech. **320**, 331–368 (1996).
[37] Dr. J. Larsson, private communication (June, 2012).
[38] A. H. Shapiro, *The Dynamics and Thermodynamics of Compressible Fluid Flow* (Ronald, 1953), Vol. 2.
[39] R. Hannappel and R. Friedrich, "Direct numerical-simulation of a Mach-2 shock interacting with isotropic turbulence," Appl. Sci. Res. **54**, 205–221 (1995).
[40] S. Lee, S. K. Lele, and P. Moin, "Interaction of isotropic turbulence with shock waves: Effect of shock strength," J. Fluid Mech. **340**, 225–247 (1997).
[41] K. Mahesh, S. K. Lele, and P. Moin, "The influence of entropy fluctuations on the interaction of turbulence with a shock wave," J. Fluid Mech. **334**, 353–379 (1997).